communications materials

Review article

https://doi.org/10.1038/s43246-024-00541-0

Hydrogels for next generation neural interfaces

Simin Cheng[1,2], Ruiqi Zhu[1,2] & Xiaomin Xu[1,2]

Overcoming the mechanical disparities between implantable neural electrodes and biological tissue is crucial in mitigating immune responses, reducing shear motion, and ensuring durable functionality. Emerging hydrogel-based neural interfaces, with their volumetric capacitance, customizable conductivity, and tissue-mimicking mechanical properties, offer a more efficient, less detrimental, and chronically stable alternative to their rigid counterparts. Here, we provide an overview of the exceptional advantages of hydrogels for the development of next-generation neural interfaces and highlight recent advancements that are transforming the field.

Neurons partake in intricate communication processes within the brain, enabling the execution of complex behaviors[1]. To understand the neuronal activities and decode the brain's working mechanism, scientific endeavor has spearheaded the development of neural probe technologies, ranging from Michigan-type to Utah-type microelectrode arrays[2,3]. The recorded electrophysiological signals distinguish by varying potential amplitude and frequencies, provide a dynamic map of the active processes within different brain regions. By detecting both low-frequency local field potential oscillations and high-frequency action potentials of single units, and performing stimulation tasks, neural electrode technologies have contributed considerably to neuroscience and biomedical engineering[4,5].

Traditional neural interfaces—based on rigid silicon (Si) or metal technologies—struggle to meet the escalating requirements for chronic applications due to their mechanical mismatch with biological tissue, chronic immune responses, and long-term function instability in biotic environment[6]. Substituting bulky and rigid materials with thin structure and softer plastic substrates has utterly improved the mechanical compliance of devices, yet hard to meet the requirements of recording stability, complete elimination of shear motion, and miniaturization of electrodes without sacrificing the signal quality. Figure 1 illustrates the development trajectory of neural interface form factors over the past five decades, highlighting how intrinsically soft and stretchable materials, notably hydrogels, with their tissue-like mechanical properties, have risen to the forefront of advanced neural technology. In this review, we first examine the inherent obstacles that persist in existing neural interface technologies, then highlight the noteworthy attributes of hydrogels, especially conductive hydrogels, and summarize their transformative potential in this sector.

The limitations in conventional neural interface technologies

Understanding the neuronal activities over a vast timescale—ranging from milliseconds to years[5,7], and thus the brain tissue's temporal progression necessitates implantable devices that exemplify exceptional long-term stability. As the neural probe navigates the landscape of multilayered brain structures, characterized by diverse Young's modulus ranging from 0.5 to 1.2 MPa for meninges[8] to 1–1.5 kPa for gray/white matter[9], conventional materials used in these devices exhibit much higher moduli–metal (~GPa), silicon (~GPa), and polymer (~MPa)[10]. The long-term implantation of rigid electrodes within soft brain tissue leads to non-uniform stress distribution at the probes-tissue interfaces[11]. Such mechanical disparity induces significant compression and shear strain, and the incongruent bending stiffness leads to undesired shear motion, altering the distribution of neurons and glial cells at the electrode interface. The non-uniform strain distribution is often exacerbated by inadequate adhesion between the electrodes and the tissue[12]. Additionally, the extended presence of neural interfaces prompts chronic immune responses, resulting in significant neuronal death and damage in the vicinity of the electrodes[1]. In response to these electronic intrusions, glial cells proliferate and assemble at the interfaces, forming an insulating glial sheath about 100 μm thick around the recording/stimulating electrodes. This gradual encapsulation of neural interfaces ultimately culminates in device failure within several months, thus shortening their lifespan[13]. Addressing this long-standing challenge[5] calls for intrinsically soft materials that have tissue-like mechanical properties and do not affect the studied system.

As a second challenge, to enable precise signal recording from single neurons and to understand the coordinated activity, high-density array should be constructed to achieve high spatial resolution in both passive and active electrodes[14,15]. Simply reducing the lateral size of Si or metal electrodes would result in increased impedance, compromising the electrodes' ability to detect low-amplitude signals due to higher background noise that potentially masks subtle signals. Moreover, the increased impedance would necessitate larger potentials to drive the currents required for effective neural stimulation, potentially affecting the integrity of the biological tissues. One should note that elevated potentials may surpass the electrochemical safety

[1]Institute of Materials Research, Shenzhen International Graduate School, Tsinghua University, Shenzhen 518055, China. [2]Shenzhen Geim Graphene Center, Tsinghua-Berkeley Shenzhen Institute, Tsinghua University, Shenzhen 518055, China. e-mail: xu.xiaomin@sz.tsinghua.edu.cn

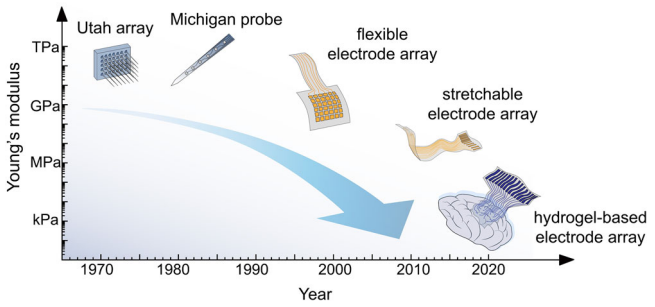

Fig. 1 | Technology roadmap for implantable neural electrodes. The evolution of neural interface technologies across decades, highlighting a transition towards enhanced device flexibility alongside a rising use of softer materials.

thresholds of the tissue, leading to adverse effects such as electrolysis, heating, or direct damage from electric fields[16]. In this perspective, optimal neural electrodes should possess low impedance to boost recording sensitivity and accurately detect the subtle electrical changes induced by neuronal activities[17]. Besides, low-impedance electrodes are preferred for stimulation due to their lower power requirements for delivering an equivalent electrical stimulus.

A common strategy is to coat the electrode surface with materials having volumetric capacitance, for instance, poly(3,4-ethylenedioxythiophene): poly(styrenesulfonate) (PEDOT:PSS), to enhance the charge injection capacity (CIC) and decrease the overall impedance[18]. PEDOT:PSS-coated platinum (Pt) electrodes have demonstrated a CIC reaching 2.71 mC cm^{-2}, in contrast to the 0.83 mC cm^{-2} CIC of non-coated Pt electrodes, under identical current pulse conditions[19]. Other strategies include substituting the electrodes with emergent materials[20,21], such as two-dimensional (2D) materials, nanofibers, conductive polymers (CPs)[22], and hydrogel in the latest innovations[23]. Materials that exhibit low impedance and high mechanical compliance are beneficial to effectively reduce the electrode size and enhance the spatial resolution of signals when used to fabricate electrode arrays. For electrodes based on flexible materials, problems of the interfacial delamination, cracks in electrodes under strain, and inherent deterioration need to be solved[24]. These undesired degradations would result in device failure typically on the sites of electrodes, reduce the lifetime and effectiveness of neural interfaces[25].

Last, the interface electronics required for amplifying, filtering, and digitizing signals from multielectrode arrays are a critical challenge in the scaling-up of such systems. Multiplexed recording sites based on semiconducting technologies can reduce the size and enhance the integration density of electrodes, yet the power consumption and dissipation of heat from active multiplexing electronics in a biotic environment is always a concern[15,26,27]. Neural interfaces built upon traditional Si-based technology, such as Neuropixels[28], Neuroseeker[29], have realized high density - 1000 channels within 0.7 mm^2 for effective subcortical activity mapping. A state-of-the-art microelectronic array constructed on polyimide (PI) allows a large-scale cortical signal mapping in moving rats, having 1024 channels in lateral dimension[30]. However, the mechanical mismatch between Si and tissues makes it unsuitable for prolonged direct contact. Additionally, rigid encapsulation is essential to shield Si-based transistors in biotic environment. An ideal neural interface device should be minimally invasive, capable of precisely targeting relevant physiological or pathological activities, and demonstrate operational stability. Organic electrolyte-gated transistors, in particular, electrochemical transistors, have inherent advantages in this regard[31].

Physio-chemical characteristics of hydrogel

Hydrogel is three-dimensional (3D) network of polymer chains, predominantly filled with water or aqueous electrolytes[32]. Broadly, hydrogels can be classified into two categories based on their origin. Natural hydrogels encompass materials such as gelatin, collagen and alginate, whereas synthetic hydrogels include substances such as polyethylene glycol (PEG) and polyvinyl alcohol (PVA), etc[33]. Given their exceptional biocompatibility, designable mechanical properties, and tunable ionic/electrical conductivity, hydrogels have drawn considerable interest across various fields. One key application lies in their use as emergent neural interfaces, serving as coating materials or as standalone electrodes that facilitate recording or stimulation. This perspective delves into how these combined characteristics shape and expand their applications in an in vivo setting.

Hydrogels, with a network of hydrophilic polymers, have tunable Young's modulus from kPa to MPa and are adaptable to multiple application scenarios. The elastic moduli of hydrogels are principally influenced by several key factors, including the type of cross-link chemistry employed, the degree of crosslinking, and the monomer or macromer concentration[34]. The latter two typically affect the elastic modulus in a predictable manner, where increased concentration or extended reaction time correlate with enhanced elastic moduli[35]. The chemistry of crosslinking, critical for polymer network formation, is categorized into chemical, dynamic, or physical crosslinking mechanisms. Among these, chemical cross-links generally possess the highest bonding energy, in contrast to the relatively lower bond energies associated with physical cross-links such as hydrogen bond[36], electrostatic force[37], inter/intra-molecular entanglement[38] or other weak bonding. The disparity in bonding energy significantly impacts the resultant elastic moduli of the hydrogels. Therefore, low elastic moduli, i.e., in the range of 10–100 kPa, can be realized through reduced cross-links density or weak polymer entanglements. The intrinsic softness of hydrogels, akin to brain tissue, then ensures their excellent conformability to the brain's intricate topography, providing stable neuron signal detection[39].

The interfacial toughness between hydrogels and tissue is also important to ensure stable attachment, as the pulsation of blood vessels and the flow of cerebrospinal fluid cause slight but continual motion of the brain, usually on the order of 2-4 μm, which imparts shear stress and mechanical strain on implanted devices[40]. An inadequate adhesion at the electrode-tissue interface could result in radial and tangential forces, causing severe shearing and compression strain to the tissue as well[12]. In this context, bio-adhesive hydrogels are particularly suitable to function as the neural interface. Currently, physical attachments yield relatively weak interfacial toughness, less than 10 J m^{-2} [38,41], mainly by electrostatic force[42] or hydrogen bonding[43]. Long-term application of neural interfaces further requests covalent anchorage between the hydrogel coating and devices[44].

Neural interfaces working in cerebrospinal fluid necessitate attention to material stability. Hydrogels, polymer networks capable of swelling in water, reach equilibrium when a balance between solvent permeation and elastic network retraction force is established[45], often resulting in volume changes. The swelling of hydrogel is not typically favored for neural interface applications, which could cause interfacial delamination, device failure, and introduce impurities to the surroundings. An increased thickness due to the hydrogel swelling may also cause local compression, pushing neurons further apart[46], altering the studying environment and reducing detection accuracy[47]. Recent research has used a substrate-constrained annealing approach to confine the swelling of hydrogel electrodes only in the vertical dimension[44,48]. The anisotropic swelling characteristic avoids the drastic shape change during long-term operation in biofluids. In other scenarios when integrated with drug delivery functions, a controllable swelling ratio is required to regulate the molecule immobilization and release processes[49].

The prerequisite for realizing effective electrophysiological sensing and optimal signal transmission is conductivity. Conductive mechanisms are generally classified into two categories: ionic conductivity and electronic conductivity. The hydrogels' mesh dimension is ~10 nm, much larger than the size of water molecules, thus allowing unrestricted mobility of ions within the matrix[50]. Ionic conductivity in hydrogels is defined as[51]:

$$\sigma = \sum_i n_i \mu_i Z_i e$$

where σ is the conductivity, n_i is the concentration of charge carriers, and μ_i denotes for ionic mobility, Z_i is the valence of mobile ion charges, and e is

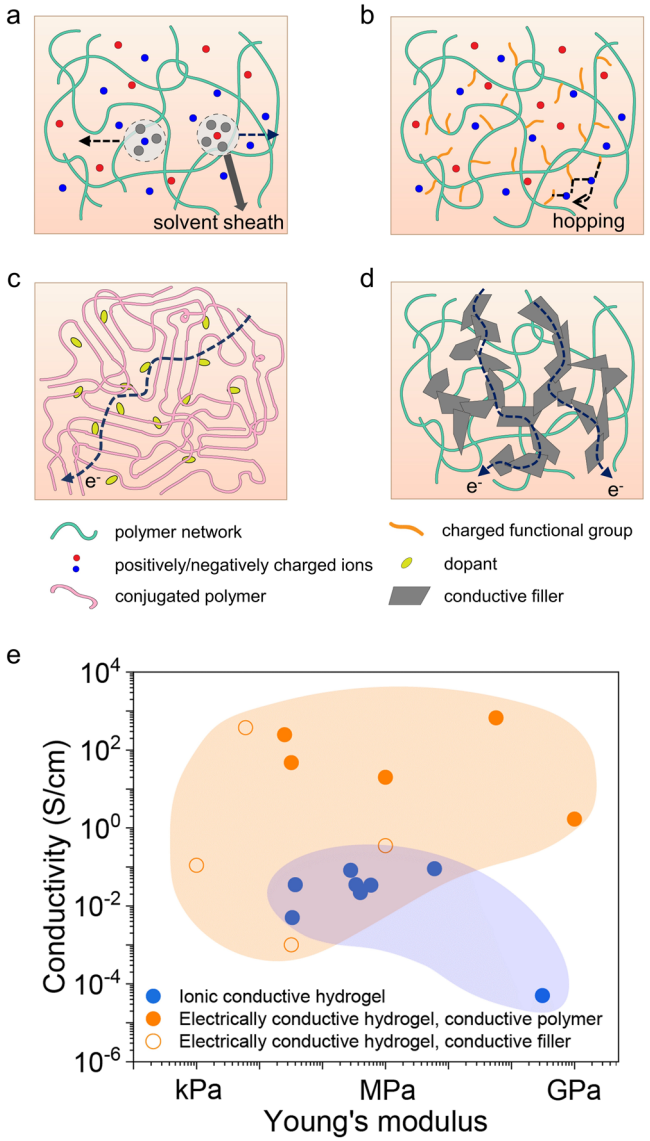

Fig. 2 | Conductive mechanisms and properties of hydrogels. a Simplified schematic of a hydrogel based on neutral 3D polymer network. The gray areas highlight the ions surrounded by water molecules, forming the hydration sheath that moves freely in an aqueous electrolyte and contributes to the conductivity. **b** Schematic of an ionic hydrogel based on a polymer having charged functional groups that facilitate the hopping of ions through polymer-electrolyte interaction and enhance the conductivity. **c** Schematic of the hydrogel based on conjugated polymer with electron transport pathways due to π-π interactions. **d** Schematic highlighting conductive fillers in electrically conductive hydrogels that facilitate electron transport. **e** Summary on the documented Young's modulus and conductivity of ionic hydrogels (blue dots)[52,54,91,93,118–121], electrically conductive hydrogels based on conductive polymers (orange dots)[32,62,89,98,100], and electrically conductive hydrogels containing conductive fillers (orange hollows)[59,69,101,102].

elementary charge, and thereby mainly dominated by n_i and μ_i. For hydrogels based on neutral 3D polymer networks, the conductivity is mainly a result of the movement of cations and anions in a hydration sheath (Fig. 2a), illustrated by hydrogels such as PVA[52]. Porous structure benefits the ionic conductivity as it decreases the hindrance to ion drifting under electric field[53–55]. Ionic hydrogels constructed by non-neutral polymer (polyanion, polycation, or polyzwitterion, etc.) backbones often show higher conductivity by leveraging polymer-electrolyte interactions (Fig. 2b). This is because the charged functional groups can immobilize the counterions and function as the hopping sites to accelerate the dissociation of cation-anion pairs[56], resulting in an enhanced conductivity. Documented ionic conductive hydrogels have an ionic conductivity mostly in the range of 10^{-5}–10^{0} S cm^{-1} [57].

Electrically conductive hydrogels can be synthesized using CPs as the primary matrix, or by incorporating conductive fillers like nanoparticles[58], carbon nanotubes[59], and graphene sheets[60] to establish charge transport pathway. For intrinsically CPs such as polypyrrole, polyaniline (PANI), and PEDOT:PSS, their conductivity primarily stems from the delocalized π-electrons transporting along the conjugated direction[61], as illustrated in Fig. 2c. Documented CP-based hydrogels have electrical conductivity ranging from 10^{0}–10^{2} S cm^{-1}, with their Young's moduli varying between 100 kPa to 1 GPa[61,62]. A conductive hydrogel can be developed by infusing crosslinking agents into the CP matrix or by substituting the ionic dopant with one that is capable for crosslinking[61]. For instance, pure PEDOT:PSS hydrogel with a high conductivity, i.e., 670 S cm^{-1}, was demonstrated, realized by controlling the distribution of PEDOT-enriched domains and forming a physical crosslinked conductive hydrogel[62].

Notably, CP-based hydrogels, known for their ionic-electronic interactions and termed as mixed ionic-electronic conductive hydrogels (MIECHs), hold significant promise for neural interface applications[63,64]. This category often comprises a water- swollen loose conjugated polymer network that can interact with ions. Upon immersion in aqueous electrolytes, MIECHs attain enhanced ionic conductivity[65], and altered electrical conductivity, driven by reversible doping-dedoping process facilitated by ionic-electronic interactions between mobile ions and conjugated backbones[66]. For example, PEDOT:PSS hydrogels, a typical MIECH, display exceptional electrical conductivity and a high CIC could show reduced conductivity in phosphate-buffered saline solution compared to in deionized (DI) water, attributed to the engagement of Na^+ ions[48]. Conversely, a PANI hydrogel infused with sulfuric acid (H_2SO_4) exhibits conductivity superior to that of either component alone[65]. This enhancement can be ascribed to ionic-electronic interactions between protons and imine nitrogens, which are diminished in the absence of water. In short, the ionic-electronic interactions, and the overall conductivity of MIECHs, are highly relevant to the specific pairing of the electrolyte and CP within the gel matrix. Selecting an appropriate hydrogel system is crucial for achieving optimal mixed ionic-electronic conductivity.

For filler-based hydrogels, it is crucial to tailor both the amount and shape/dimension of the fillers to approach the percolation threshold efficiently[67,68]. Studies suggest that nanowire-shaped fillers outperform nanospheres in achieving lower percolation thresholds (Fig. 2d). Documented filler-based hydrogels possess electrical conductivity in the range of 10^{-5}–10^{2} S cm^{-1}, and elastic moduli varying between 1 kPa to 10 MPa (Fig. 2e)[61,69]. One should not that incorporating an excessive amount of fillers into hydrogels could compromise their mechanical compliance due to the undesired local aggregation of these fillers. Conversely, maintaining a moderate filler content within the hydrogel can preserve its low Young's modulus. However, this balance is achieved at the expense of reducing the material's conductivity[59]. The biocompatibility of filler-based hydrogels depend on both the polymer matrix and filler materials used. While metal nanoparticles exhibit superior conductivity, their long-term implantation in the saline conditions can result in hydrolysis and corrosion. These processes could lead to local inflammation and a decrease in the detection capabilities[70].

In the context of neural interface applications, biocompatibility serves as a crucial criterion in searching for suitable materials. The porous structure and low elastic modulus of hydrogels endow them an inherent compatibility with tissues, offering mechanical properties closely resembling those of natural tissues. This compatibility is further enhanced using biocompatible components, including natural polymers like gelatin and alginate, or polymerized macromolecules such as PEG and PVA, which ensure the cytocompatibility of the hydrogels. Moreover, the surface chemistry of hydrogels significantly affects the biocompatibility through the absorption of proteins via functional groups, such as hydrophilic surfaces or charged groups. This, in turn, influences the interactions between cells and materials[71]. CP-based hydrogels can exhibit exceptional tissue biocompatibility and

cytocompatibility, with protein absorption facilitated by the electrostatic forces of their charged backbones[64].

Bio-adhesive hydrogels as the surface coating on neural electrodes

The incorporation of a conductive hydrogel coating onto metallic or Si microelectrodes results in notable enhancement in their electrochemical properties, including reduced impedance, increased CIC, and enhanced charge storage capability, compared to their performance when composed solely of bare metal[72]. Moreover, hydrogel coatings applied to neural electrodes can act as a bio-adhesive interface, providing a mechanical cushioning that ensures a stable contact with tissue, and in some scenarios facilitating targeted drug delivery for modulation of the neural activity[73,74]. These coatings significantly enhance the integration stability of the neural electrodes, improving the fidelity of the recorded signals[12]. For implantable electronics monitoring large, dynamic tissues—such as multiple brain regions[40], the heart[43], the bladder[75], or dorsal subcutaneous area[76]—interfaces, not only the hydrogel/tissue interface, but also the electrode/hydrogel interface (Fig. 3a), with more robust bonding are essential for long-term stability. For such scenarios, interfaces should endure substantial movement without detachment, ensuring continuous function even amid organ deformation.

Devices that are securely anchored and feature stabilized hydrogel coating/electrode and hydrogel/tissue interfaces exhibit improved signal integrity and temporal resolution[76,77]. Such resilient interfaces can be realized through covalent bonding or chemical anchoring methods. To enhance the interfacial robustness between the metal electrode and the hydrogel coating layer, the electrode surface can be pre-treated with molecules having reactive carbon-carbon double bonds[78,79], enabling reaction with monomer precursors of the hydrogel. For instance, gold (Au) electrodes were functionalized with N, N′-bis(acryloyl) cystamine (BAC) to react with the C=C bonds in acrylamide in the PEDOT:PSS ink. The resulting acrylamide/PEDOT:PSS conductive hydrogel can adhere strongly to electrodes, reducing interfacial delamination[79]. In another approach, a polymerized poly(styrene sulfonate-co-4-vinyl pyridine) (PSS-4VP) backbone was anchored on an acrylate-functionalized metallic electrodes, followed by coating of a CP, i.e., 3,4-ethylenedioxythiophene (EDOT)[23], yielding an interfacially bonded PEDOT:Poly (SS-4VP) hydrogel, which is conductive. This robust hydrogel coating maintains its bond even after sonication. Alternative methods include adding an extra adhesive and conductive layer to enhance the hydrogel-electrode adhesion[80].

Adhesion of hydrogel coatings to tissue is usually achieved through covalent bonding[81]. Unlike the pretreatment required for metal electrodes, tissue naturally contains functional groups on its surface, such as amino groups, eliminating the need for pre-treatments. Sulfated N-hydroxysuccinimide has been incorporated in hydrogel to promote the formation of covalent bonds with amino groups on the tissue surface. This creates a robust interface, supporting continuous optical stimulation of the dorsal subcutaneous area for an extended period, up to a week[76]. Incorporating catechol groups, such as dopamine, into the polymer network creates a denser array of hydrogen bonds, yielding a more robust interface[82,83]. A prototype featuring Si micro-shanks coated with a 15 ± 5 μm-thick poly (vinyl acetate) (PVA) hydrogel exhibited a four- to fivefold reduction in stress from micromotion, attributed to the exceptional adhesive properties of PVA to tissue[84].

Finally, hydrogel coatings on neural electrodes provide a dual function by serving as vehicles for targeted drug delivery[85]. Their porous structure and tunable biodegradable nature allow therapeutic molecules to be delivered and released in a controllable manner to the target sites[86]. For instance, hydrogel consisting of lactic acid units in the polymer chains can realize a finely tuned release rate because of its controllable biodegradation rate[87]. Leveraging such biodegradable hydrogels, modulators such as neural growth factor, brain-derived neurotrophic factor, and neurotrophins can be delivered to modulate activities in targeted neural regions precisely.

Conductive hydrogels as neural electrodes

Hydrogels having high conductivity and tissue-like mechanical properties are ideal for use as recording or stimulation electrodes in neural interfaces. The regulation of physiological functions, including cognition, learning, and memory, relies on the transmission of signals within individual cells and the synaptic communications among neuron networks. These behaviors are associated with neurotransmitter dynamics and electrochemical processes, specifically the modulation of cell membrane potentials driven by the movement of ions, known as polarization and depolarization processes.

Ionically conductive hydrogels utilize mobile ions or ion-conductive substances as signal transmission pathways, mirroring the mechanisms employed by living tissues, thus enabling effective communication with neural tissues[88]. Commonly used methodologies for the fabrication of ionically conductive hydrogels often involve immersing the polymer matrix in an ionic solution to induce the ion exchange, thereby increasing the ion concentration within the hydrogel. This practice typically begins with the crosslinking or pre-crosslinking of the polymer matrix such as PVA, PEG, or a blend of polyacrylamide and alginate (PAAm-alginate), etc. Subsequently, the crosslinked matrix is immersed into ionic solutions containing ions such as Ca^{+}, Na^{+}, Al^{3+}, Cl^{-}, causing ions to diffuse into the polymer matrix due to the concentration gradient[52,89,90]. The ionic conductivity of these hydrogels can be controlled by adjusting the salt concentration, the duration and temperature of the immersion, etc. The polymer matrix crosslinked in advance does not obstruct the ion-conduction pathway, thus the conductivity of such hydrogels mainly depends on the ion concentration[91].

Incorporating ionically conductive materials, such as ionic solutions (e.g., LiCl)[92] or ionic liquids[93], into hydrogel precursors is another strategy to enhance ionic conductivity. The ionic conductivity of a hydrogel infused with a highly concentrated LiCl solution can be increased by up to 90 times (reaching 89.9 mS cm^{-1}) compared to that of a deionized hydrogel (1 mS cm^{-1})[91]. Hydrogels formulated with ionic liquids and crosslinkers have the potential for improved functionality and extended stability when properly encapsulated[94]. While elevating the ion concentration can significantly increase the ionic conductivity of hydrogels, raising from 10^{-5} S cm^{-1} to 10^{0} S cm^{-1} [95–97], it is crucial to consider these levels in the context of physiological ion concentrations, typically below 300 mM. Unusually high ion concentrations (exceeding 1 M) within ionically conductive hydrogels may create a concentration gradient. This scenario could trigger ion exchanges between hydrogels and the surrounding tissue media, potentially impacting the electrical stability of the implanted devices and posing risks to the biological environment at the implantation site[61].

Electrically conductive hydrogels can exhibit superior properties for rapid biological response and precise in vivo neuromodulation. CP-based hydrogels are notable for their biocompatibility and robustness in biotic environments. In particular, conductive hydrogels comprising PEDOT:PSS have attracted considerable attention due to their mixed electrical and ionic conductivity, and biocompatibility. Zhou et al. developed a bicontinuous CP-based hydrogel by controlling the ratio of PEDOT: PSS and hydrophilic polyurethane (PU), achieving a high conductivity exceeding 11 S cm^{-1} [32]. Chong et al. [98] reported a template-directed assembly method, that facilitates the growth of ultrathin PEDOT:PSS fiber networks along poly acrylic acid (PAA) chains, forming a continuous conductive network within the hydrogel, and producing an impressive conductivity of 247 S cm^{-1}. Sulfuric acid or ionic liquids with strong ionic polarity were introduced to break the electrostatic interaction between the positively charged PEDOT and the negatively charged PSS, allowing the reorganization of PEDOT chains (Fig. 3b)[99]. With improved π-π interaction among the PEDOT domains, the electrical conductivity of pure PEDOT:PSS hydrogel reached 47.4 ± 1.2 S cm^{-1} [100]. An alternative approach uses laser to induce the phase separation, providing PEDOT-rich continuous phase and boosting the conductivity of PEDOT:PSS hydrogel to 670 S cm^{-1} [62]. Recent advancements have used the conductive fillers such as silver (Ag) nanosheets, to further enhance the conductivity to 374 S cm^{-1} [101]. Avoiding irregular dispersion of conductive fillers in the hydrogel matrix helps promote a continuous conductive network, for instance, controlling 2D carbon

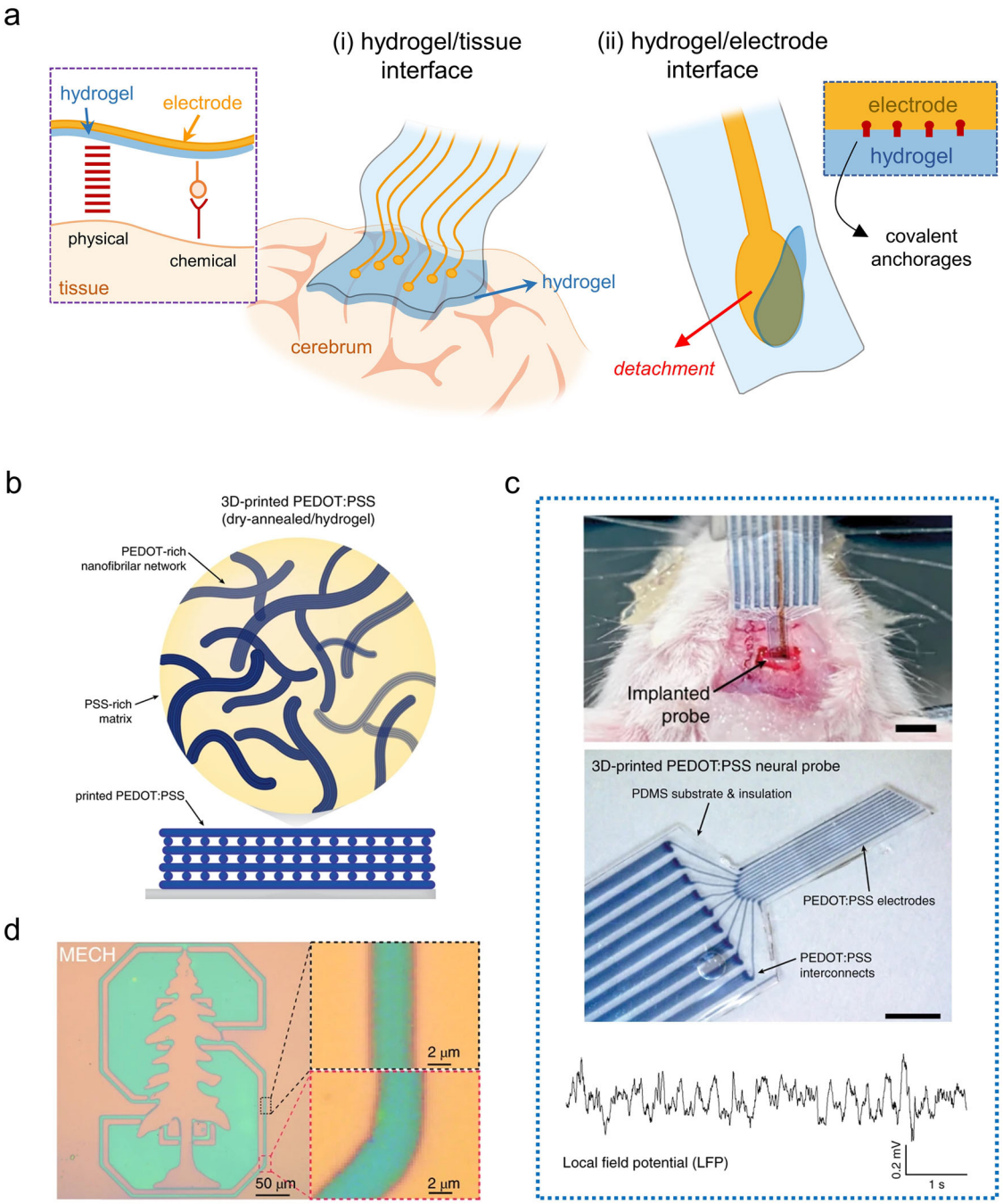

Fig. 3 | Hydrogel as the neural interface. a Schematic showing the physical attachment and chemical anchorage at (i) the hydrogel/tissue interface and (ii) the hydrogel/electrode interface. **b** Schematic showing the 3D-printed conducting PEDOT:PSS hydrogel. **c** 3D-printed PEDOT:PSS neural electrodes implanted to a free-moving mouse, and the local field potential (bottom) recorded from the freely-moving mouse. **d** Photopatterned electrically conductive hydrogel reaching a high resolution of 5 µm (left panel), with straight and curved lines resolved (right panels). **b**, **c** are reproduced with permission from ref. 99. Copyright: Springer-Nature, 2020. **d** is reproduced with permission from ref. 100 Copyright: Springer-Nature, 2019.

nanomaterials highly oriented via fluid flow in polymer matrix while extruding from the nozzle during 3D printing[102].

Emergent applications scenarios

With combined features of high conductivity and low impedance at 1 kHz, mechanical compliance and biocompatibility, conductive hydrogels have found extensive use in emergent neural interfaces, including neural signal recording, electrical stimulation, and other functions[61]. For example, pure PEDOT:PSS hydrogels[62] and hydrogels with carbon nanomaterials[69] have been utilized in recording neural signals from bullfrogs and mice, and shown ability as stimulating electrodes. PEDOT:PSS hydrogels[100] and hydrogels with Ag nanosheets[103] were used as stimulation electrodes, both evoked a higher motor response in the hind limbs of mice compared to that achieved by their reference electrodes, i.e., conventional platinum electrodes.

Next-generation neural interfaces necessitate the development of electrode arrays with enhanced spatiotemporal resolution. This advanced resolution is pivotal for achieving a comprehensive mapping of the neural activity, facilitating in-depth analysis of neuronal interactions across multiple brain regions. Additionally, high-resolution arrays can deliver finely localized stimulation to specific neurons or designated neuronal

regions, allowing effective treatments for neurodegenerative disorders. However, patterning continuous hydrogel electrodes over a large scale at sub-100-μm resolution remains challenging using traditional lithography and etching methods, given the highly porous structure and water content in hydrogels. Using 3D printing, a 9-channel electrode array with a size of 30 μm for each electrode was realized based on PEDOT:PSS conductive hydrogel[99]. In another approach, with an intermediate ion gel state, which transforms into a hydrogel after a water exchange process, Bao et al. made photolithographic patterning possible for hydrogel, and successfully reduced the linewidth down to 5 μm (Fig. 3d)[100]. The resulting micropatterned hydrogels maintain advantages of high electrical conductivity ($47.4 \pm 1.2\ S\ cm^{-1}$), low Young's modulus of 32 ± 5.1 kPa, a current-injection density ~30 times higher than that of platinum electrodes, and stable electrical performance under strain[100].

Finally, effectively maintaining a neural implant over the long term is an ongoing challenge, yet quite essential for monitoring the progression of neurological diseases, studying the neural plasticity and the brain's ability to adapt its structure over time in response to new experiences, learning, or injury recovery[104]. Hydrogel-based neural electrodes have shown potential for long-term applications[105]. For instance, PEDOT:PSS/PU electrodes were implanted to the rat heart, rat sciatic nerve, and spinal cord, and demonstrated capability of recording signals after 4 weeks and stimulating the rat spinal cord after 8 weeks of implantation[32]. An epidural electrocorticography (ECoG) electrode constructed using supramolecular β-peptide-based hydrogel realized an effective implantation for 6 weeks (Fig. 3e)[106]. A hybrid probe with PAAm-alginate hydrogel encapsulation allowed tracking of isolated single neuron potentials in freely-moving mice over 6 months following the implantation[107].

Hydrogels as the electrolyte in organic transistors

Organic transistors have inherent advantages for detecting low-amplitude signals at physiologically relevant time scales, due to their inherent amplification capabilities and capability for in-situ signal processing[108]. Conventional organic field effect transistors (OFETs) require relatively high input voltage (in the order of tens of volts) to switch on, and are often susceptible to water or ion penetration damage and must be fully encapsulated to ensure chronic use in physiologic environments[109]. Electrolyte-gated OFETs[110] and organic electrochemical transistors (OECTs)[111] liberate such limitations with their channel directly contacting the electrolyte solution. Despite this, substantial challenges persist in broadening their applications, most notably being severe crosstalk and insufficient stability[112]. The main concern is that the electrolyte is an integral part of the transistor, and ions in the electrolyte are shared by all device units on the same supporting substrate. In this regard, hydrogels, especially hydrogels with excellent capability of patterning, offer unique advantages in future construction of bioelectronic circuits for in vivo applications[113,114]. In recent studies, OECTs based on hydrogel electrolyte demonstrated transconductance (g_m) values comparable to the counterpart devices based on liquid electrolyte[111], reaching 16 mS[115].

Outlook

Of the many materials discovered to optimally combine mechanical compliance and biocompatibility, hydrogels stand out. Highly conductive hydrogels having low impedance in vivo, tunable adhesiveness, and stability in biotic environment are especially promising to replace traditional metal electrodes for chronic applications. To meet the rigorous requirements demanded by chronic neural interfaces, the composition and structural design of hydrogels must be approached with precision.

As a surface coating material, hydrogels with optimal biocompatibility and interfacial adhesiveness requires the selection of safe, washable monomers equipped with functional groups capable of forming robust, long-lasting bonds with tissues or metallic electrodes. The mechanical properties of hydrogels can be finely tuned through both compositional and structural modifications. Generally, a more loosely arranged polymer network is recommended to mimic the softness of brain tissue and accommodate the dynamics of in vivo movements[5].

In the context of using hydrogels as standalone neural electrodes, enhancing conductivity represents the foremost challenge in current materials development efforts. The conductive of hydrogels relies on the strategic configuration of conductive pathways. For filler-based hydrogels, the selection and distribution engineering of conductive fillers, the integration between these fillers and hydrogel matrix, and the densification of the polymer network all account[101]. For developing pure CP-based hydrogels and MIECHs, strategies are focused on creating a 3D continuous polymer network through ionic crosslinkers or employing reswelling strategies to dissolve soluble polymeric chains, thereby forming an entangled chain network. Such meticulous design ensures the conductive hydrogels meet the demands of detecting low-amplitude neural signals, while maintaining their mechanical conformability.

To fully exploit the benefits of hydrogels in future neural interfaces, several technical challenges must be addressed including high-throughput fabrication, programmable patterning, and facile integration[116]. Furthermore, integrating surface ECoG electrodes with deep-brain electrodes could yield extensive insights by correlating the diverse activities and functions within brains, and enable establish closed-loop feedback mechanisms. Research into hydrogel-based deep-brain neural electrodes is still in its preliminary stage. Hydrogel fibers exhibiting adaptive bending stiffness controlled by the hydration states were reported[107]. Further engineering into vertical multielectrode arrays would offer greater spatial resolution in depth. Looking ahead, there is an increasing need to develop multifunctional neural interfaces capable of high spatiotemporal resolution recording, in-situ processing, and suited for long-term implantation. Leveraging the customizable properties of hydrogels could pave the way for innovative form factors in neural interfaces, creating potential to significantly deepen our understanding of neural networks, and unravel the mysteries of the brain[117].

Received: 28 November 2023; Accepted: 4 June 2024;
Published online: 12 June 2024

References

1. Polikov, V. S., Tresco, P. A. & Reichert, W. M. Response of brain tissue to chronically implanted neural electrodes. *J. Neurosci. Methods* **148**, 1–18 (2005).
2. Wise, K. D., Angell, J. B. & Starr, A. An integrated-circuit approach to extracellular microelectrodes. *IEEE Trans. Biomed. Eng.* **3**, 238–247 (1970).
3. Campbell, P. K., Jones, K. E. & Normann, R. A. A 100 electrode intracortical array: structural variability. *Biomed. Sci. Instrum.* **26**, 161–165 (1990).
4. Buzsáki, G., Anastassiou, C. A. & Koch, C. The origin of extracellular fields and currents—EEG, ECoG, LFP and spikes. *Nat. Rev. Neurosci.* **13**, 407–420 (2012).
5. Hong, G. & Lieber, C. M. Novel electrode technologies for neural recordings. *Nat. Rev. Neurosci.* **20**, 330–345 (2019).
6. Chen, R., Canales, A. & Anikeeva, P. Neural recording and modulation technologies. *Nat. Rev. Mater.* **2**, 1–16 (2017).
7. Araki, T. et al. Flexible neural interfaces for brain implants—the pursuit of thinness and high density. *Flex. Print. Electron.* **5**, 043002 (2020).
8. Minev, I. R. et al. Electronic dura mater for long-term multimodal neural interfaces. *Science* **347**, 159–163 (2015).
9. Budday, S. et al. Mechanical properties of gray and white matter brain tissue by indentation. *J. Mech. Behav. Biomed. Mater.* **46**, 318–330 (2015).
10. Liu, X., Liu, J., Lin, S. & Zhao, X. Hydrogel machines. *Mater. Today* **36**, 102–124 (2020).
11. Kozai, T. D. Y. et al. Mechanical failure modes of chronically implanted planar silicon-based neural probes for laminar recording. *Biomaterials* **37**, 25–39 (2015).
12. Subbaroyan, J., Martin, D. C. & Kipke, D. R. A finite-element model of the mechanical effects of implantable microelectrodes in the cerebral cortex. *J. Neural Eng.* **2**, 103 (2005).

13. Sridharan, A., Rajan, S. D. & Muthuswamy, J. Long-term changes in the material properties of brain tissue at the implant–tissue interface. *J. Neural Eng.* **10**, 066001 (2013).
14. Berényi, A. et al. Large-scale, high-density (up to 512 channels) recording of local circuits in behaving animals. *J. Neurophysiol.* **111**, 1132–1149 (2014).
15. Patolsky, F. et al. Detection, stimulation, and inhibition of neuronal signals with high-density nanowire transistor arrays. *Science* **313**, 1100–1104 (2006).
16. Scholvin, J. et al. Close-packed silicon microelectrodes for scalable spatially oversampled neural recording. *IEEE Trans. Biomed. Eng.* **63**, 120–130 (2015).
17. Schiavone, G. et al. Guidelines to study and develop soft electrode systems for neural stimulation. *Neuron* **108**, 238–258 (2020).
18. Chik GKK et al. Flexible multichannel neural probe developed by electropolymerization for localized stimulation and sensing. *Adv. Mater. Technol.* **7**, 2200143 (2022).
19. Green, R. & Abidian, M. R. Conducting polymers for neural prosthetic and neural interface applications. *Adv. Mater.* **27**, 7620–7637 (2015).
20. Viswam, V., Obien MEJ, Franke, F., Frey, U. & Hierlemann, A. Optimal electrode size for multi-scale extracellular-potential recording from neuronal assemblies. *Front. Neurosci.* **13**, 385 (2019).
21. Zeng, Q. & Huang, Z. Challenges and opportunities of implantable neural interfaces: from material, electrochemical and biological perspectives. *Adv. Funct. Mater.* **33**, 2301223 (2023).
22. Jiang, Y. et al. Topological supramolecular network enabled high-conductivity, stretchable organic bioelectronics. *Science* **375**, 1411–1417 (2022).
23. Zhang, J. et al. Engineering electrodes with robust conducting hydrogel coating for neural recording and modulation. *Adv. Mater.* **35**, 2209324 (2023).
24. Oldroyd, P. & Malliaras, G. G. Achieving long-term stability of thin-film electrodes for neurostimulation. *Acta Biomater.* **139**, 65–81 (2022).
25. Barrese, J. C. et al. Failure mode analysis of silicon-based intracortical microelectrode arrays in non-human primates. *J. Neural Eng.* **10**, 066014 (2013).
26. Tian, B. et al. Three-dimensional, flexible nanoscale field-effect transistors as localized bioprobes. *Science* **329**, 830–834 (2010).
27. Kruskal, P. B., Jiang, Z., Gao, T. & Lieber, C. M. Beyond the patch clamp: nanotechnologies for intracellular recording. *Neuron* **86**, 21–24 (2015).
28. Jun, J. J. et al. Fully integrated silicon probes for high-density recording of neural activity. *Nature* **551**, 232–236 (2017).
29. Raducanu, B. C. et al. Time multiplexed active neural probe with 1356 parallel recording sites. *Sensors* **17**, 2388 (2017).
30. Chung, J. E. et al. High-density, long-lasting, and multi-region electrophysiological recordings using polymer electrode arrays. *Neuron* **101**, 21–31.e25 (2019).
31. Xu, W., Wang, J., Cheng, S. & Xu, X. Flexible organic transistors for neural activity recording. *Appl. Phys. Rev.* **9**, 031308 (2022).
32. Zhou, T. et al. 3D printable high-performance conducting polymer hydrogel for all-hydrogel bioelectronic interfaces. *Nat. Mater.* **22**, 895–902 (2023).
33. Lee, K. Y. & Mooney, D. J. Hydrogels for tissue engineering. *Chem. Rev.* **101**, 1869–1880 (2001).
34. Yuk, H. et al. Dry double-sided tape for adhesion of wet tissues and devices. *Nature* **575**, 169–174 (2019).
35. Oyen, M. L. Mechanical characterisation of hydrogel materials. *Int. Mater. Rev.* **59**, 44–59 (2014).
36. Xu, L. et al. A solvent−exchange strategy to regulate noncovalent interactions for strong and antiswelling hydrogels. *Adv. Mater.* **32**, 2004579 (2020).
37. Peng, F., Li, G., Liu, X., Wu, S. & Tong, Z. Redox-responsive gel−sol/sol−gel transition in poly (acrylic acid) aqueous solution containing Fe (III) ions switched by light. *J. Am. Chem. Soc.* **130**, 16166–16167 (2008).
38. Baumgartner, M. et al. Resilient yet entirely degradable gelatin-based biogels for soft robots and electronics. *Nat. Mater.* **19**, 1102–1109 (2020).
39. Lacour, S. P., Courtine, G. & Guck, J. Materials and technologies for soft implantable neuroprostheses. *Nat. Rev. Mater.* **1**, 16063 (2016).
40. Muthuswamy J., Saha R., Gilletti A. Tissue micromotion induced stress around brain implants. In *Proc. 3rd IEEE/EMBS Special Topic Conference on Microtechnology in Medicine and Biology*) (IEEE, 2005).
41. Cheng, S. et al. Ultrathin hydrogel films toward breathable skin−integrated electronics. *Adv. Mater.* **35**, 2206793 (2023).
42. Lei, Z., Zhu, W., Zhang, X., Wang, X. & Wu, P. Bio−inspired ionic skin for theranostics. *Adv. Funct. Mater.* **31**, 2008020 (2021).
43. Choi, H. et al. Adhesive bioelectronics for sutureless epicardial interfacing. *Nat. Electron.* **6**, 779–789 (2023).
44. Deng, J. et al. Electrical bioadhesive interface for bioelectronics. *Nat. Mater.* **20**, 229–236 (2021).
45. Syed, K. H. G., Saphwan, A.-A., Glyn, O. P. Hydrogels: methods of preparation, characterisation and applications. *Progress in Molecular and Environmental Bioengineering* (ed Angelo, C) (IntechOpen, 2011).
46. Thavarajah, D., De Lacy, P., Hussain, R. & Redfern, R. M. Postoperative cervical cord compression induced by hydrogel (DuraSeal): a possible complication. *Spine* **35**, E25–E26 (2010).
47. Kim, D.-H., Wiler, J. A., Anderson, D. J., Kipke, D. R. & Martin, D. C. Conducting polymers on hydrogel-coated neural electrode provide sensitive neural recordings in auditory cortex. *Acta Biomater.* **6**, 57–62 (2010).
48. Lu, B. et al. Pure PEDOT: PSS hydrogels. *Nat. Commun.* **10**, 1043 (2019).
49. Li, J. & Mooney, D. J. Designing hydrogels for controlled drug delivery. *Nat. Rev. Mater.* **1**, 16071 (2016).
50. Yang, C. & Suo, Z. Hydrogel ionotronics. *Nat. Rev. Mater.* **3**, 125–142 (2018).
51. Xu, K. Nonaqueous liquid electrolytes for lithium-based rechargeable batteries. *Chem. Rev.* **104**, 4303–4418 (2004).
52. Zhou, Y. et al. Highly stretchable, elastic, and ionic conductive hydrogel for artificial soft electronics. *Adv. Funct. Mater.* **29**, 1806220 (2019).
53. Dechiraju, H., Jia, M., Luo, L. & Rolandi, M. Ion−conducting hydrogels and their applications in bioelectronics. *Nat. Commun.* **6**, 2100173 (2022).
54. Wang, K. et al. Chemically crosslinked hydrogel film leads to integrated flexible supercapacitors with superior performance. *Adv. Mater.* **27**, 7451–7457 (2015).
55. Barros, W. Jr Solvent self-diffusion dependence on the swelling degree of a hydrogel. *Phys. Rev. E* **99**, 052501 (2019).
56. Han, S. et al. Sequencing polymers to enable solid-state lithium batteries. *Nat. Mater.* **22**, 1515–1522 (2023).
57. Peng, Q. et al. Recent advances in designing conductive hydrogels for flexible electronics. *InfoMat* **2**, 843–865 (2020).
58. Dvir, T. et al. Nanowired three-dimensional cardiac patches. *Nat. Nanotechnol.* **6**, 720–725 (2011).
59. Shin, S. R. et al. Carbon-nanotube-embedded hydrogel sheets for engineering cardiac constructs and bioactuators. *ACS nano* **7**, 2369–2380 (2013).
60. Annabi, N. et al. Highly elastic and conductive human-based protein hybrid hydrogels. *Adv. Mater.* **28**, 40–49 (2016).
61. Yuk, H., Lu, B. & Zhao, X. Hydrogel bioelectronics. *Chem. Soc. Rev.* **48**, 1642–1667 (2019).
62. Won, D. et al. Digital selective transformation and patterning of highly conductive hydrogel bioelectronics by laser-induced phase separation. *Sci. Adv.* **8**, eabo3209 (2022).

63. Bianchi, M. et al. Poly (3, 4−ethylenedioxythiophene) −based neural interfaces for recording and stimulation: fundamental aspects and in vivo applications. *Adv. Sci.* **9**, 2104701 (2022).
64. Heo, D. N. et al. Development of 3D printable conductive hydrogel with crystallized PEDOT:PSS for neural tissue engineering. *Mater. Sci. Eng.* **99**, 582–590 (2019).
65. Stejskal, J. et al. Mixed electron and proton conductivity of polyaniline films in aqueous solutions of acids: beyond the 1000 S cm^{-1} limit. *Polym. Int.* **58**, 872–879 (2009).
66. Paulsen, B. D., Tybrandt, K., Stavrinidou, E. & Rivnay, J. Organic mixed ionic–electronic conductors. *Nat. Mater.* **19**, 13–26 (2020).
67. Guo, Y. et al. Hydrogels and hydrogel-derived materials for energy and water sustainability. *Chem. Rev.* **120**, 7642–7707 (2020).
68. Wang, G., Wang, C., Zhang, F. & Yu, X. Electrical percolation of nanoparticle-polymer composites. *Comput. Mater. Sci.* **150**, 102–106 (2018).
69. Tringides, C. M. et al. Viscoelastic surface electrode arrays to interface with viscoelastic tissues. *Nat. Nanotechnol.* **16**, 1019–1029 (2021).
70. Doering, M., Kieninger, J., Urban, G. A. & Weltin, A. Electrochemical microelectrode degradation monitoring: in situ investigation of platinum corrosion at neutral pH. *J. Neural Eng.* **19**, 016005 (2022).
71. Chen, H., Yuan, L., Song, W., Wu, Z. & Li, D. Biocompatible polymer materials: role of protein—surface interactions. *Prog. Polym. Sci.* **33**, 1059–1087 (2008).
72. Inoue, A., Yuk, H., Lu, B. & Zhao, X. Strong adhesion of wet conducting polymers on diverse substrates. *Sci. Adv.* **6**, eaay5394 (2020).
73. Bettinger, C. J. et al. Recent advances in neural interfaces—materials chemistry to clinical translation. *MRS Bull.* **45**, 655–668 (2020).
74. Proctor, C. M. et al. Ionic hydrogel for accelerated dopamine delivery via retrodialysis. *Chem. Mater.* **31**, 7080–7084 (2019).
75. Li, G. et al. Highly conducting and stretchable double−network hydrogel for soft bioelectronics. *Adv. Mater.* **34**, 2200261 (2022).
76. Yang, Q. et al. Photocurable bioresorbable adhesives as functional interfaces between flexible bioelectronic devices and soft biological tissues. *Nat. Mater.* **20**, 1559–1570 (2021).
77. Liu, J. et al. Intrinsically stretchable electrode array enabled in vivo electrophysiological mapping of atrial fibrillation at cellular resolution. *Proc. Natl Acad. Sci.* **117**, 14769–14778 (2020).
78. Yuk, H., Zhang, T., Lin, S., Parada, G. A. & Zhao, X. Tough bonding of hydrogels to diverse non-porous surfaces. *Nat. Mater.* **15**, 190–196 (2016).
79. Shur, M. et al. Soft printable electrode coating for neural interfaces. *ACS Appl. Bio. Mater.* **3**, 4388–4397 (2020).
80. Yang, M. et al. Poly (5-nitroindole) thin film as conductive and adhesive interfacial layer for robust neural interface. *Adv. Funct. Mater.* **31**, 2105857 (2021).
81. Forssell M., et al. Compliant adhesive cuff electrode for selective stimulation in rat vagus nerve. In *Proc. IEEE Sensors Conference* (IEEE, 2019).
82. Huang, W. C. et al. Ultracompliant hydrogel−based neural interfaces fabricated by aqueous−phase microtransfer printing. *Adv. Funct. Mater.* **28**, 1801059 (2018).
83. Wang, X. et al. Bioadhesive and conductive hydrogel-integrated brain-machine interfaces for conformal and immune-evasive contact with brain tissue. *Matter* **5**, 1204–1223 (2022).
84. Sridharan, A., Nguyen, J. K., Capadona, J. R. & Muthuswamy, J. Compliant intracortical implants reduce strains and strain rates in brain tissue in vivo. *J. Neural Eng.* **12**, 036002 (2015).
85. Abidian, M. R. & Martin, D. C. Multifunctional nanobiomaterials for neural interfaces. *Adv. Funct. Mater.* **19**, 573–585 (2009).
86. Yue, Z., Moulton, S. E., Cook, M., O'Leary, S. & Wallace, G. G. Controlled delivery for neuro-bionic devices. *Adv. Drug Deliv. Rev.* **65**, 559–569 (2013).
87. Winter, J. O., Gokhale, M., Jensen, R. J., Cogan, S. F. & Rizzo, I. I. I. J. F. Tissue engineering applied to the retinal prosthesis: Neurotrophin-eluting polymeric hydrogel coatings. *Mater. Sci. Eng.* **28**, 448–453 (2008).
88. Zhao, Z., Spyropoulos, G. D., Cea, C., Gelinas, J. N. & Khodagholy, D. Ionic communication for implantable bioelectronics. *Sci. Adv.* **8**, eabm7851 (2022).
89. Ji, D. et al. Superstrong, superstiff, and conductive alginate hydrogels. *Nat. Commun.* **13**, 3019 (2022).
90. Zhao, S. et al. Programmable hydrogel ionic circuits for biologically matched electronic interfaces. *Adv. Mater.* **30**, 1800598 (2018).
91. Wang, S. et al. Strong, tough, ionic conductive, and freezing-tolerant all-natural hydrogel enabled by cellulose-bentonite coordination interactions. *Nat. Commun.* **13**, 3408 (2022).
92. Pan, L. et al. A compliant ionic adhesive electrode with ultralow bioelectronic impedance. *Adv. Mater.* **32**, 2003723 (2020).
93. Noshadi, I. et al. Engineering biodegradable and biocompatible bio-ionic liquid conjugated hydrogels with tunable conductivity and mechanical properties. *Sci. Rep.* **7**, 4345 (2017).
94. Ren, Y. et al. Ionic liquid-based click-ionogels. *Sci. Adv.* **5**, eaax0648 (2019).
95. Schroeder, T. B. et al. An electric-eel-inspired soft power source from stacked hydrogels. *Nature* **552**, 214–218 (2017).
96. Kim, C.-C., Lee, H.-H., Oh, K. H. & Sun, J.-Y. Highly stretchable, transparent ionic touch panel. *Science* **353**, 682–687 (2016).
97. Keplinger, C. et al. Stretchable, transparent, ionic conductors. *Science* **341**, 984–987 (2013).
98. Chong, J. et al. Highly conductive tissue-like hydrogel interface through template-directed assembly. *Nat. Commun.* **14**, 2206 (2023).
99. Yuk, H. et al. 3D printing of conducting polymers. *Nat. Commun.* **11**, 1604 (2020).
100. Liu, Y. et al. Soft and elastic hydrogel-based microelectronics for localized low-voltage neuromodulation. *Nat. Biomed. Eng.* **3**, 58–68 (2019).
101. Ohm, Y. et al. An electrically conductive silver–polyacrylamide–alginate hydrogel composite for soft electronics. *Nat. Electron.* **4**, 185–192 (2021).
102. Zhang, M. et al. Microribbons composed of directionally self-assembled nanoflakes as highly stretchable ionic neural electrodes. *Proc. Natl Acad. Sci.* **117**, 14667–14675 (2020).
103. Hui, Y. et al. Three-dimensional printing of soft hydrogel electronics. *Nat. Electron.* **5**, 893–903 (2022).
104. Patel, S. R. & Lieber, C. M. Precision electronic medicine in the brain. *Nat. Biotechnol.* **37**, 1007–1012 (2019).
105. Fu, T.-M. et al. Stable long-term chronic brain mapping at the single-neuron level. *Nat. Methods* **13**, 875–882 (2016).
106. Nam, J. et al. Supramolecular peptide hydrogel-based soft neural interface augments brain signals through a three-dimensional electrical network. *ACS Nano* **14**, 664–675 (2020).
107. Park, S. et al. Adaptive and multifunctional hydrogel hybrid probes for long-term sensing and modulation of neural activity. *Nat. Commun.* **12**, 3435 (2021).
108. Khodagholy, D. et al. High transconductance organic electrochemical transistors. *Nat. Commun.* **4**, 2133 (2013).
109. Fang, H. et al. Ultrathin, transferred layers of thermally grown silicon dioxide as biofluid barriers for biointegrated flexible electronic systems. *Proc. Natl Acad. Sci.* **113**, 11682–11687 (2016).
110. Knopfmacher, O. et al. Highly stable organic polymer field-effect transistor sensor for selective detection in the marine environment. *Nat. Commun.* **5**, 2954 (2014).
111. Khodagholy, D. et al. In vivo recordings of brain activity using organic transistors. *Nat. Commun.* **4**, 1575 (2013).
112. Li, N. et al. Bioadhesive polymer semiconductors and transistors for intimate biointerfaces. *Science* **381**, 686–693 (2023).
113. Lee, H. et al. Ultrathin organic electrochemical transistor with nonvolatile and thin gel electrolyte for long−term

electrophysiological monitoring. *Adv. Funct. Mater.* **29**, 1906982 (2019).
114. Bihar, E. et al. Self-healable stretchable printed electronic cryogels for in-vivo plant monitoring. *npj Flex. Electron.* **7**, 48 (2023).
115. Han, S. et al. Ion transport to temperature and gate in organic electrochemical transistors with anti-freezing hydrogel. *Org. Electron.* **108**, 106605 (2022).
116. Sagdic, K., Fernández-Lavado, E., Mariello, M., Akouissi, O. & Lacour, S. P. Hydrogels and conductive hydrogels for implantable bioelectronics. *MRS Bull.* **48**, 495–505 (2023).
117. Khodagholy, D., Ferrero, J. J., Park, J., Zhao, Z. & Gelinas, J. N. Large-scale, closed-loop interrogation of neural circuits underlying cognition. *Trends Neurosci.* **45**, 968–983 (2022).
118. Huang, H. et al. Multiple stimuli responsive and identifiable zwitterionic ionic conductive hydrogel for bionic electronic skin. *Adv. Electron. Mater.* **6**, 2000239 (2020).
119. Song, X. et al. A tunable self-healing ionic hydrogel with microscopic homogeneous conductivity as a cardiac patch for myocardial infarction repair. *Biomaterials* **273**, 120811 (2021).
120. Kong, W. et al. Muscle−inspired highly anisotropic, strong, ion −conductive hydrogels. *Adv. Mater.* **30**, 1801934 (2018).
121. Gan, S. et al. Hydroxypropyl cellulose enhanced ionic conductive double-network hydrogels. *Int. J. Biol. Macromol.* **181**, 418–425 (2021).

Acknowledgements

The authors acknowledge support from Ministry of Science and Technology of the People's Republic of China (No. 2023YFE0101400), National Natural Science Foundation of China (No. 52273249 & 52003141), Natural Science Foundation of Guangdong Province (No. 2021A1515010493 & 2021ZT09L197), Shenzhen Science and Technology Innovation Commission (Nos. RCYX20210609103710028, WDZC20200818092033001, and KQTD20210811090112002), and Shenzhen Geim Graphene Center.

Author contributions

X.X. conceived the topic and supervised the research. X.X., S.C. and R.Z. wrote the manuscript. All authors discussed and revised the manuscript.

Competing interests

The authors declare no competing interests.

Additional information

Supplementary information The online version contains supplementary material available at https://doi.org/10.1038/s43246-024-00541-0.

Correspondence and requests for materials should be addressed to Xiaomin Xu.

Peer review information *Communications Materials* thanks the anonymous reviewers for their contribution to the peer review of this work. Primary Handling Editors: Maria Rosa Antognazza and John Plummer. A peer review file is available.